Potential anticorrosive effect of hexamethylenediamine Penta(methylphosphonic) acid on c-steel in hydrochloric acid Solution: An experimental study with DFTB and molecular dynamics simulations

H. Bouammali[1*], E.H. Loukili[2], H. Elmsellem[1,3], S. Jerdioui[1], K. Bekkouch[1], A. Aouniti[1], R. Salghi[3,4], C. Jama[5], F. Bentiss[5,6], B. Hammouti[2,7]

[1] *Laboratory of Applied Chemistry and Environment (LCAE). Department of Chemistry, Faculty of Sciences, University Mohamed I, Oujda, Morocco*
[2] *Euro-Mediterranean University of Fes, P.O. Box 15, 30070 Fez, Morocco*
[3] *Higher Institute of Nursing Professions and Health Techniques (ISPITSO), Oujda 63303, Morocco.
Laboratory of Applied Chemistry and Environment (LCAE) sciences faculty, Oujda, Morocco.*
[4] *Laboratory of Applied Chemistry and Environment, ENSA, University Ibn Zohr, Agadir 80000, Morocco*
[5] *Univ. Lille, CNRS, INRAE, Centrale Lille, UMR8207 - UMET - Unité Matériaux et Transformations, F-59000 Lille, France*
[6] *Laboratoire de Catalyse et de Corrosion des Matériaux (LCCM), Faculté des Sciences, Université Chouaib Doukkali, B.P. 20, M-24000 El Jadida, Morocco*
[7] *Laboratory of Industrial Engineering, Energy and The Environment (LI3E) SUPMTI Rabat, Morocco*

*For Corresponding author: Email address: e.loukili@ueuromed.org (E. Loukili)

Abstract: The inhibition ability of Hexamethylenediamine penta(methylphosphonic) acid (HTMP) against carbon steel corrosion in 1 M HCl at 30°C was evaluated by weight loss, electrochemical (potentiodynamic and electrochemical impedance spectroscopy, EIS) methods. The experimental results showed that HTMP was a good inhibitor for the steel corrosion in 1 M HCl medium and its inhibition efficiency increased with the inhibitor concentration. Data, obtained from ac impedance measurements, were analyzed to model the corrosion inhibition process through appropriate equivalent circuit models. Adsorption of HTMP on the carbon steel surface followed the Langmuir adsorption isotherm. Surface analysis by (SEM) supported the formation of a protective inhibitor film on the carbon steel surface. Furthermore, the theoretical study was carried out using the density functional theory (DFT) method. DFTB calculations revealed that inhibitor molecules formed covalent bonds with iron atoms, which was confirmed by the Projected Density of States (PDOS) of adsorbed systems.

Keywords: Organic phosphonic acid; Carbon steel; Hydrochloric acid; Corrosion Inhibition; Adsorption.

1. Introduction

Utilizing corrosion inhibitors represents a highly cost-effective strategy for reducing corrosion rates, safeguarding metal surfaces against corrosion, and preserving industrial facilities, particularly in acidic environments. Extensive research has been conducted on the inhibition of steel corrosion in acid solutions, focusing on various types of organic inhibitors. Among these, environmentally

friendly inhibitors such as N-heterocyclic organic compounds, including triazoles (El Issami *et al.,* 2007), oxadiazoles (Raviprabha *et al.,* 2023), thiadiazoles (Liu *et al.,* 2023), pyrazoles (Timoudan *et al.,* 2023; Azgaou *et al.,* 2022), purines (Mihajlović *et al*., 2019), imidazopyridine (Ech-chihbi *et al.,* 2016; Salim *et al.,* 2021), benzimidazole (Chkirate *et al*., 2021), aldehydes (Lazrak *et al.,* 2022) pyridazines (Bentiss *et al.,* 2012),...), as well as p and o-phosphates/poly-phosphates, are preferred [Nakayama *et al.,* 2000; Prabakaran *et al*., 2014; Moumeni *et al*., 2020; Naderi *et al.,* 2009; Yang *et al.,* 2010; Liu *et al.,* 2017; Lebrini *et al.,* 2019; Souissi *et al.,* 2008; Askari *et al.,* 2014). Additionally, the protective properties of organic phosphonic acids against corrosion in various media, including their application as water treatment agents due to low toxicity, high stability, and corrosion inhibition activity in neutral aqueous environments, have been extensively explored by researchers (Salah *et al.,* 2017; Amar *et al.,* 2006; Tabti *et al.,* 2020; Laamari *et al.,* 2011; Dalmoro *et al.,* 2019; Dalmoro *et al.,* 2012; Kinlen *et al.,* 2002; Rao *et al.,* 2013; laamari *et al.,* 2010; Prabakaran *et al.,* 2013; Prabakaran *et al.,* 2014).

Building on our previous research concerning the development of organic phosphonic acids as corrosion inhibitors in acidic media (Labjar *et al.,* 2011; Bouammali *et al.,* 2015), we investigated the corrosion inhibiting performance of a novel organic phosphonic acid specifically, Hexamethylenediamine penta(methylphosphonic) acid (HTMP) on carbon steel in a 1 M HCl medium at 30°C. The selection of this compound was based on considerations of its molecular structure, with HTMP featuring multiple phosphonic functional groups and heteroatoms (nitrogen). To assess the inhibition properties of HTMP on carbon steel corrosion in 1 M HCl, we employed weight loss measurements and electrochemical impedance spectroscopy (EIS) techniques.

2. Experimental details
2.1. Materials

The tested compound, namely Hexamethylenediamine penta(methylphosphonic) acid (HTMP) solutions, was obtained from Sigma-Aldrich chemical co. and its chemical structure is presented in **Fig. 1.** The material used in this study was a carbon steel (Euronorm: C35E carbon steel and US specification: SAE 1035) with a chemical composition (in wt%) of 0.370% C, 0.230% Si, 0.680% Mn, 0.016% S, 0.077% Cr, 0.011% Ti, 0.059% Ni, 0.009% Co, 0.160% Cu and the remainder iron (Fe). The steel samples were pre-treated prior to the experiments by grinding with emery paper SiC (120, 400, 600 and 1200); rinsed with distilled water, degreased in acetone in an ultrasonic bath immersion for 5 min, washed again with bidistilled water and then dried at room temperature before use. The acid solutions (1 M HCl) were prepared by dilution of an analytical reagent grade 37% HCl with double distilled water. The concentration range of HTMP employed in this study was 10^{-6} M–10^{-2} M.
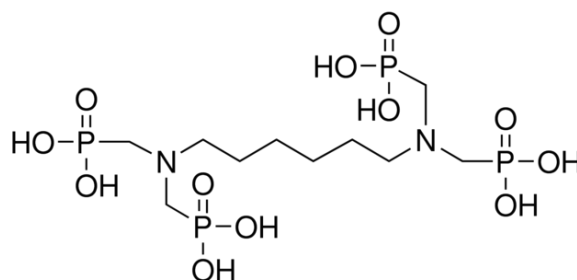

Figure. 1. Chemical structure of the investigated organic phosphonic acid (HTMP).

2.2. Corrosion tests

The gravimetric measurements were carried out at the definite time interval of 24 h at room temperature (30 °C) using an analytical balance (precision 0.1 mg). The steel specimens used had a rectangular form (length = 5 cm, width = 2 cm, thickness = 0.3 cm).

Gravimetric experiments were carried out in a double glass cell equipped with a thermostated cooling condenser containing 250 ml of non-de-aerated test solution.

After immersion period, the steel specimens were withdrawn, carefully rinsed with bidistilled water, ultrasonically cleaned in acetone, dried at room temperature and then weighed. Triplicate experiments were performed in each case and the average value of the weight loss was used to calculate the corrosion rate (C_R) in mg/cm^2.h and the inhibition efficiency $\eta_{WL}(\%)$ in percent (%). These were calculated from Eqs. (1) and (2) (Bentiss *et al.,* 2012; Bouklah *et al.,* 2006; Hbika *et al.,* 2023), respectively:

$$C_R = \frac{W_b - W_a}{A_t} \qquad (1)$$

$$\eta_{WL}\% = \left(1 - \frac{W_i}{W_0}\right) \times 100 \qquad (2)$$

In this context, W_b and W_a represent the weight of the specimen before and after immersion in the tested solution, W_0 and W_i denote the corrosion weight losses of carbon steel in uninhibited and inhibited solutions, respectively. A stand for the total area of the steel specimen (measured in square centimeters), and t indicates the exposure time (measured in hours).

Impedance tests under alternating current were conducted in a polymethylmethacrylate (PMMA) cell with a 1000 ml capacity, maintained at a temperature of 30±1°C using a thermostat. A saturated calomel electrode (SCE) served as the reference electrode, and a platinum leaf was utilized as the counter electrode. All potentials were referenced against SCE. The working electrode, fashioned from a square carbon steel sheet, exposed an area of 7.55 cm^2 to the solution. Impedance spectra were recorded at the steady state of open circuit potential, specifically at the corrosion potential, following 24 hours of the working electrode's exposure to the solution (no deaeration, no stirring). AC impedance measurements were conducted employing a potentiostat Solartron SI 1287, a Solartron 1255B frequency response analyzer, and ZPlot 2.80 software for test execution and data collection. The electrochemical system's response to AC excitation, covering a frequency range from 10^5 Hz to 10^{-2} Hz, and a peak-to-peak amplitude of 10 mV was measured with a data density of 10 points per decade. All electrochemical impedance spectroscopy (EIS) diagrams were recorded at the open circuit potential, i.e., the corrosion potential (E$_{corr}$). Typically, one EIS spectrum was recorded within a 10-minute timeframe. The impedance data were analyzed and fitted using ZView 2.80, an equivalent circuit software simulation.

3. Results and Discussion
3.1. Corrosion inhibition
3.1.1. *Evaluation Gravimetric tests*

The corrosion rate (C$_R$) and the inhibition efficiency, $\eta_{WL}(\%)$, values obtained from weight loss method at different concentrations of HTMP after 24 h of immersion in 1 M HCl at 30°C were given in **Table 1.** It is obvious from these results that along with the increase of HTMP concentration, the values of C$_R$ decrease gradually, i.e. the corrosion of steel was retarded by HTMP, or the inhibition

was enhanced by the inhibitor concentration. Indeed, the variation in $n_\%$ with concentration of HTMP, presented in **Figure 2**, showed that the protection inhibition efficiency increased with the increase of the HTMP concentration, the maximum η_{WL} (%) of 95% was achieved at 10^{-2} M after 24 h of immersion in 1 M HCl. Noticeably, when the concentration of HTMP was less than 510^{-3} M, η_{WL} increased sharply with an increase in concentration, but a further raise inhibitor concentration caused no appreciable change in inhibitive performance. This behaviour can be due to the fact that the adsorption coverage of inhibitor on steel surface increases with the inhibitor concentration. The good inhibitive performance of HTMP may be explained on the basis of adsorption of the HTMP molecules (physisorption and/or chemisorption). The HTMP molecules can be easily protonated to form cation–ionic forms in HCl solution and therefore adsorb at the metal surface through the already adsorbed chloride ions. Also, the adsorption of the neutral HTMP molecules could occur through to the formation of links between the d-orbital of iron atoms, involving the displacement of water molecules from the metal surface, and the lone sp^2 electron pairs present on the N, P and O atoms and π-orbitals in phosphonic functional group, blocking the active sites in the steel surface and therefore decreasing the corrosion rate.

Table 1. Corrosion parameters obtained from weight loss measurements for carbon steel in 1 M HCl containing various concentrations of HTMP at 30°C.

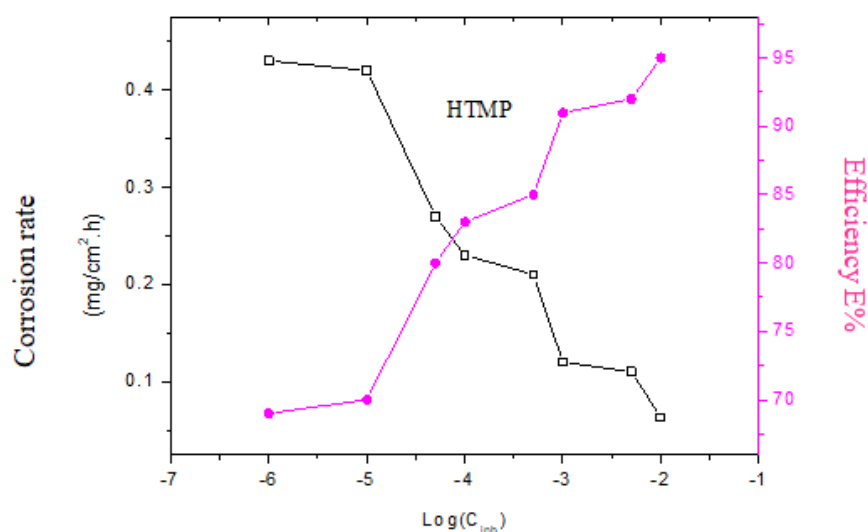| Inhibiteur	Concentration	C_R (mg/cm^2.h)	$\eta_{WL}\%$
Blanc	1M	1.39	-
HTMP	10^{-6}	0.43	69
	10^{-5}	0.42	70
	510^{-5}	0.27	80
	10^{-4}	0.23	83
	510^{-4}	0.21	85
	10^{-3}	0.12	91
	510^{-3}	0.11	92
	10^{-2}	0.063	95

Figure 2. Evolution of inhibitory efficiency and corrosion rate as a function of HTMP concentration

3.1.2. Electrochemical Study
3.1.2.1. Potentiostatic Study

Figure 3 depict the evolution of potentiostatic curves $E_{corr}=f(t)$ during the first 60 minutes of immersion. According to these curves, we observe that the potential becomes increasingly noble with the rise in inhibitor concentration.
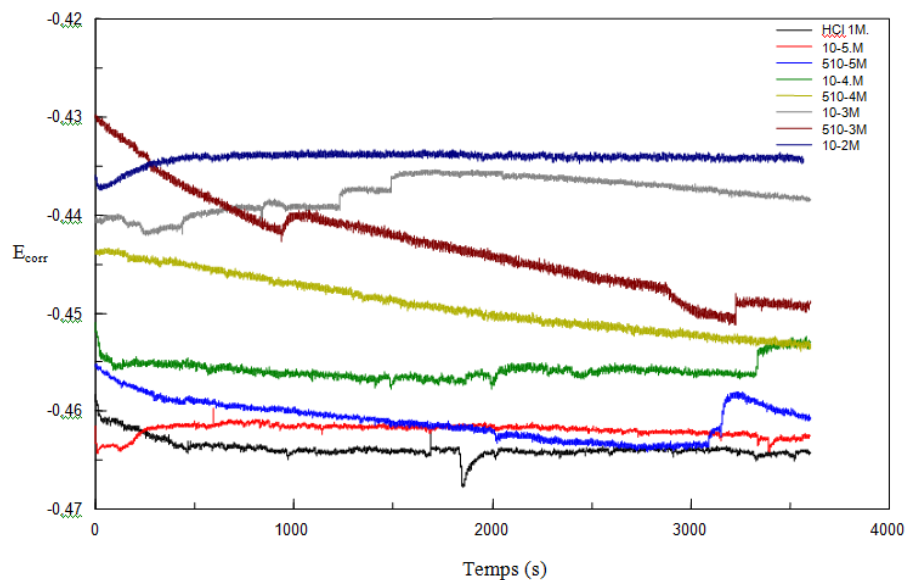

Figure 3. Potentiostatic curves $E_{corr} = f(t)$ as a function of HTMP concentration.

This shift is attributed to the delayed anodic dissolution reaction of iron caused by the action of the HTMP molecule. The value of E_{corr} varies minimally over time, and fluctuations in potential, primarily towards more negative potentials, are observed. These fluctuations can be attributed to local breaches in the film on the electrode surface.

3.1.2.2. Polarization Curves
- **Effect of Concentration**

In the potentiostatic method, the electrode potential is stabilized during a one-hour immersion before proceeding with the measurements of the I=f(E) curves. The polarization curves in the absence and presence of HTMP, at various concentrations, in a 1M HCl medium at 30°C, are shown in **Figure 4.** The shape of the Log I = f(E) curves as a function of HTMP concentration is essentially identical. The examination of **Figure 4** shows that in the cathodic domain, the addition of HTMP induces a significant decrease in the cathodic partial current. The cathodic reaction involves the reduction of the hydrogen cation in two successive steps. We observe that the cathodic curves appear as Tafel lines, indicating that the hydrogen reduction reaction on the steel surface follows a mechanism of pure activation. The addition of HTMP to the corrosive environment results in a slight modification of the slopes of the Tafel lines (**Table 2**). This result leads us to suggest that the proton reduction mechanism (slower step) is not altered by the addition of the HTMP inhibitor (Aksüt *et al.,* 1982). In the anodic domain, the action of HTMP results in a decrease in currents. The values of corrosion current densities (I_{corr}), corrosion potential, cathodic and anodic Tafel slopes (ßc and ßa), and inhibition efficiency (E%) for various concentrations of HTMP in 1M HCl medium are reported in **Table 2.**
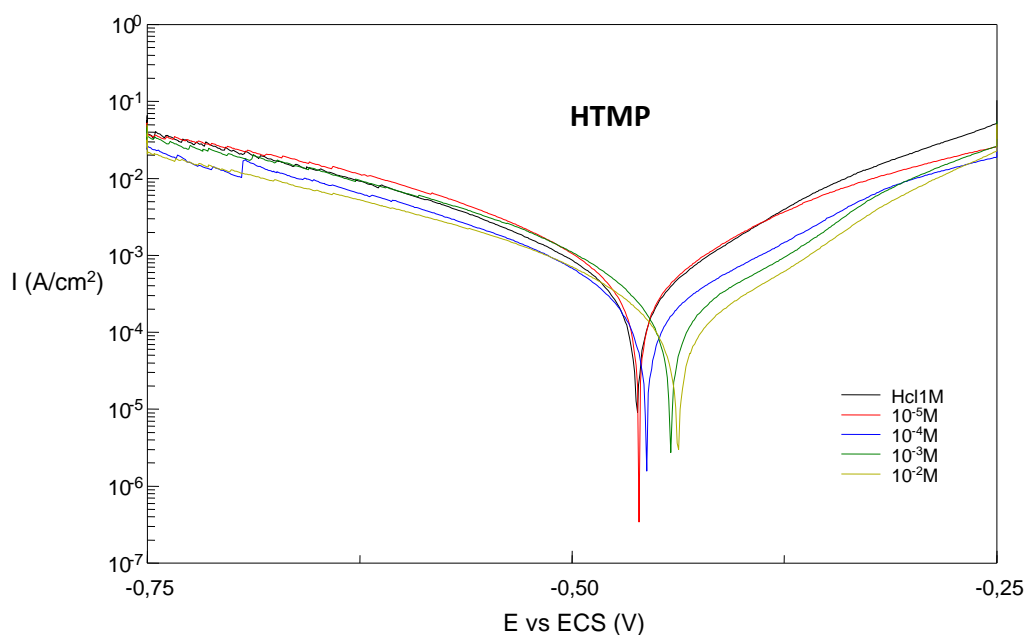
Figure 4. Polarization curves of steel in 1M HCl without and with the addition of various concentrations of HTMP.

Table 2. Electrochemical parameters and inhibitory efficiency of steel corrosion in 1M HCl, with and without the addition of various concentrations of HTMP at 30°C.

Inhibitor	C (M)	β_a mV.dec^{-1}	β_c mV.dec^{-1}	E_{corr} Vs(ESC) (mV)	I_{corr} μA/cm^2	E(%)	θ
HCl	1M	97	134	-462	537	--	--
HTMP	10^{-5}	110	90	-462	305	43	0,43
	10^{-4}	102	96	-456	247	54	0,54
	10^{-3}	80	66	-442	160	70	0,7
	10^{-2}	80	81	-438	119	79	0,79

According to the results obtained in the table, it can be concluded that the polarization curves analysis confirms the inhibitory nature of HTMP on the corrosion of steel, as previously observed through weight loss measurements. The Corrosion current densities (I_{corr}) decrease as the concentration of HTMP increases, along with a corresponding decrease in corrosion rates. The addition of HTMP slightly modifies the E_{corr} values, and we observe that the inhibitory efficiency (E %) increases with the rise in inhibitor concentration. Moreover, in the anodic domain, the presence of HTMP leads to a reduction in oxidation current densities. This result clearly indicates that HTMP has both cathodic and anodic effects. Therefore, HTMP can be classified as mixed inhibitors in hydrochloric acid 1M medium.

- *Effect of Temperature*

The effect of temperature on the acid-surface reaction of steel is highly complex, as numerous changes can occur on the metal surface, such as rapid etching and inhibitor desorption. Additionally, the inhibitor itself may undergo decomposition and/or rearrangement. To determine the effect of

temperature on the inhibitory efficiency of the studied molecule HTMP, we plotted polarization curves of steel in 1M HCl both with and without the addition of HTMP, within the temperature range of 30-60°C. **Figures 5** and **6** depict the temperature effect on the cathodic and anodic polarization curves of steel in 1M HCl, both in the absence and presence of 10^{-2}M HTMP.
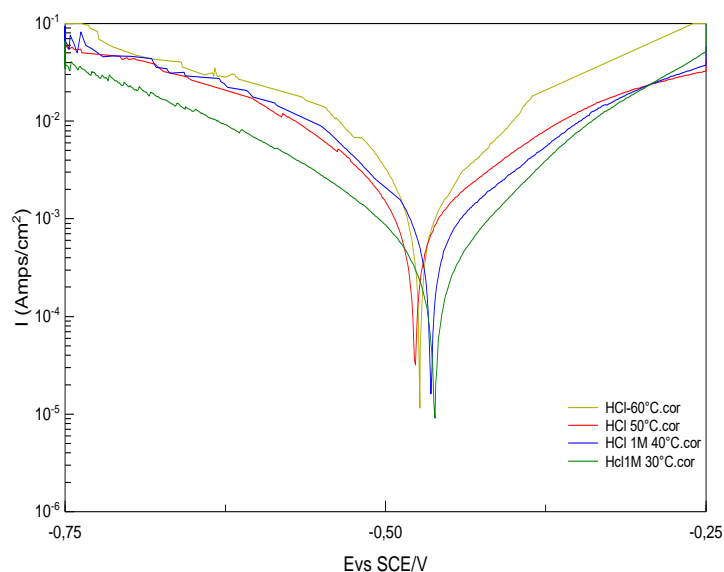

Figure 5. Effect of Temperature on Cathodic and Anodic Polarization Curves of Steel in 1M HCl.
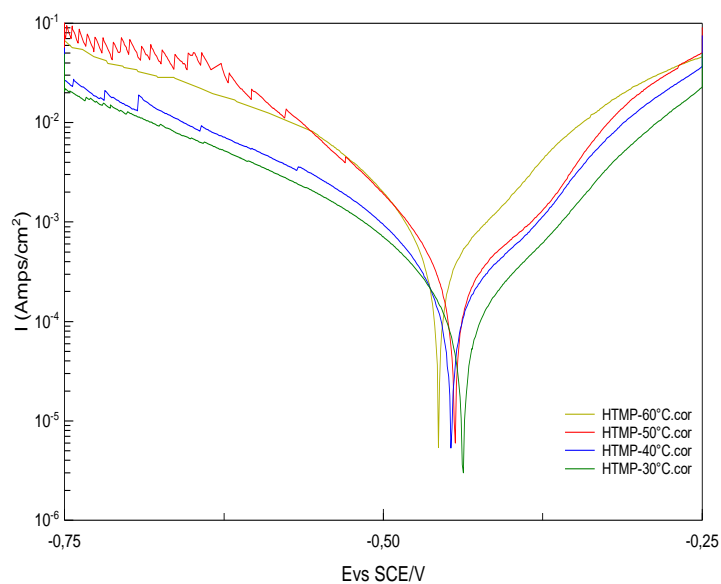

Figure 6. Effect of Temperature on Cathodic and Anodic Polarization Curves of Steel in 1M HCl in the Presence of 10^{-2}M HTMP.

Based on the results obtained, the following observations can be noted:

1) In the cathodic domain, current densities increase with the rise in temperature from 30 to 60°C, exhibiting nearly the same trend. This suggests that the reduction of H^+ at the surface of the steel occurs through a pure activation mechanism across the entire temperature range studied.

2) The corrosion potential of the steel (E_{corr}) is altered by the increase in temperature from 30 to 60°C in 1M HCl both with and without the addition of HTMP.

The values of corrosion current densities (Icorr), corrosion potentials of the steel (Ecorr), and the inhibitory efficiency of HTMP as a function of temperature are provided in **Table 3**. In general, it is observed that the increase in temperature leads to an increase in Icorr, and the inhibitory efficiency rises across the entire temperature range studied. Singh et al suggests that the temperature increase results in an augmentation of electron density around the adsorption centers, explaining the attainment of the highest inhibitory efficiency value (Kaur *et al.,* 2008; Bammou *et al.,* 2010, Hamid *et al.*, 2022). The coverage ratio (θ) is calculated using the following relationship (Khamis *et al.,* 1990):

$$I_{corr\ (inh)} = (1-\theta)I_{corr} + \theta I_{sat} \tag{3}$$

Rearranging this equation yields:

$$\theta = \left(\frac{I_{corr} - I_{corr(inh)}}{I_{corr} - I_{sat}} \right) \tag{4}$$

where Icorr, Icorr(inh), and Isat are the corrosion current density values of the steel determined by extrapolating the cathodic Tafel lines after immersion in an acidic medium, respectively, without and with the addition of HTMP. When the surface is fully covered, ($I_{corr} = I_{sat}$ for the highest concentration). As $I_{sat} << I_{corr}$

$$\theta = \left(\frac{I_{corr} - I_{corr(inh)}}{I_{corr}} \right) \tag{5}$$

Table 3. Influence of Temperature on the Electrochemical Parameters of Steel in 1M HCl + 10^{-2}M HTMP Environment.

inhibitor	Temperature °C	Ecorr Vs SCE (mV)	Icorr (µA/cm²)	E%	θ
1M HCl	30	-462	537	-	-
	40	-464	1077	-	-
	50	-477	1527	-	-
	60	-473	2929	-	-
HTMP	30	-438	119	79	0.79
	40	-447	190	82	0.82
	50	-445	275	82	0.82
	60	-457	560	81	0.81

In general, the values of Icorr increase with temperature, whether or not an inhibitor is present in the solution (**Table 3**). The evolution of corrosion currents in the corrosive solution shows a steady and rapid growth, confirming an increasing metal dissolution with the rise in temperature. Hence, there is a slight decrease in inhibitory efficiency with increasing temperature. The relationship between corrosion rate and temperature is represented by the Arrhenius equation (Belghiti *et al.,* 2020; Hmamou *et al.,* 2015):

$$I_{corr} = K \exp\left(\frac{-E_a}{RT} \right) \tag{6}$$

Where E_a is the activation energy, and K is a constant.

Figure 7 illustrates the variation of the logarithm of the corrosion current density as a function of the inverse of the absolute temperature. This variation of Ln $(I_{corr})=f(1/T)$ forms a straight line both without and with the addition of the HTMP inhibitor at 10^{-2}M. The activation energies from the Arrhenius relationship, both without and with the addition of the HTMP inhibitor in 1M HCl, are provided in **Table 4.** We observe a slight increase in activation energies for HTMP compared to the blank (1M HCl).
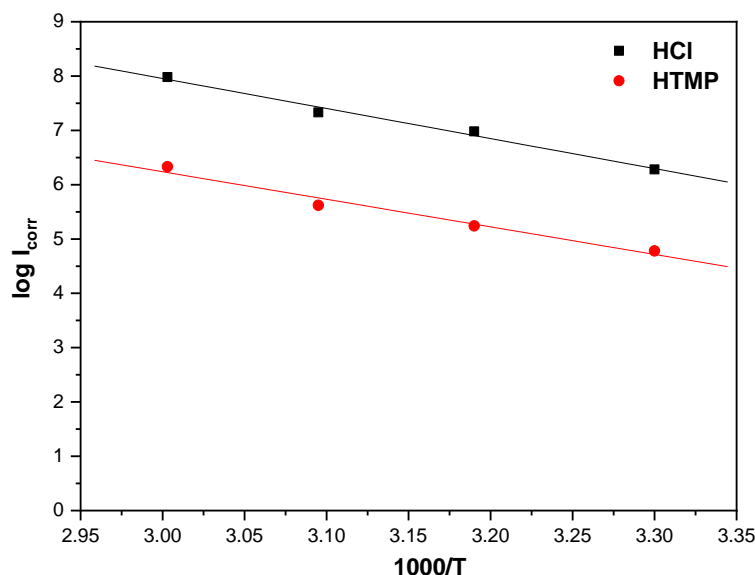

Figure 7. Arrhenius lines calculated based on the corrosion current density of steel in 1M HCl + HTMP at 10^{-2}M

Table 4. Activation energy of steel in HCl medium without and with the addition of HTMP.

	1M HCl	**10^{-2} M of HTMP**
E_a (kJ/mol)	45	49

3.1.2.3. Ac impedance study

The electrochemical impedance diagrams are recorded at the corrosion potential for various concentrations and immersion times. The surface area of the counter electrode (CE) steel is 7.66 cm^2.

- *Effect of HTMP concentration*

The Nyquist diagram and Bode diagram of the steel immersed in acidic solutions, with and without the addition of various concentrations of HTMP, are presented in **Figure 8** and **9.** These diagrams are obtained after 24 hours of immersion at the corrosion potential. The impedance response of carbon steel in acidic solution changed significantly after the addition of HTMP, and the size of the semicircle increases with the inhibitor concentration, indicating that the inhibitory effect also increases for both compounds. The impedance spectra manifest as a capacitive loop at high frequency (HF) with a single time constant detected in the Bode plots. The capacitive loop observed in the highest frequency range is generally attributed to the double-layer relaxation during charge-discharge, representing a very rapid process (Ashassi-Sorkhabi *et al.,* 2006).

At high concentration, the emergence of a low-frequency inductive loop became evident, especially at 10^{-2} M of HTMP (**Figure 8** and **9**). The presence of the low-frequency inductive loop

can be attributed to the relaxation of adsorbed species on the electrode surface, such as Cl^-_{ads} and H^+_{ads} (Amin *et al.,* 2007; Lenderink *et al.,* 1993; Veloz *et al.,* 2002). It may also be associated with the adsorption of the inhibitor on the electrode surface (Morad *et al.,* 2000) or the re-dissolution of the passivated surface at low frequencies (Sherif *et al.,* 2006). On the other hand, the low-frequency inductive behavior is likely due to the stabilization of the layer formed by the corrosion reaction products on the electrode surface (e.g., $[FeOH]_{ads}$ and $[FeH]_{ads}$), involving inhibitor molecules and their reaction products (Kelly *et al.,* 1965).

Figure 10 represents the equivalent electrical circuit of the HTMP compound adsorption, while for HTMP, poor fitting is observed for concentrations of 10^{-3} and 10^{-2}M. **Figure 11** and **12** illustrates the adjusted Nyquist and Bode diagrams for 10^{-2}M of HTMP. It was evident that, in these cases, the best fit cannot be achieved using the same simple model (a), and additional elements are required. Indeed, data analysis revealed that the impedance diagrams of HTMP (at concentrations of 10^{-3} and 10^{-2}M) consist of a large capacitive loop at high frequency (HF), followed by a smaller capacitive loop at low frequency (LF). The first larger HF capacitive loop can be attributed to a charge transfer process, while the second smaller LF loop may be linked to the adsorption of HTMP molecules on the metallic surface and/or to other substances accumulated at the metal/interface (inhibitor molecules, corrosion products, etc.) (Solmaz *et al.,* 2008). In this case, model (a) in **Figure 10** is insufficient to describe the electrochemical impedance spectra in the presence of 10^{-3} and 10^{-2}M HTMP. The alternative model (b) with two-time constants is depicted in the same figure. This model has allowed for the determination of adsorption parameters such as R_a and CPE_a (A_a and n_a, respectively). In **Figure 10**, R_s represents the solution resistance, R_{ct} is the charge transfer resistance, and CPE_d represents the capacitance of the high-frequency semicircle attributed to the charge transfer process. R_a represents the resistance of adsorbed HTMP molecules, and CPE_a is the capacitance of the film formed by the adsorption of these compounds on the steel surface.

Figure 11 and **12** illustrates an example of the Nyquist and relative Bode fitting obtained with the circuit model from **Figure 10**. It can be observed that the proposed model of the spectra for the studied compound is representative of the indicated phenomena, either at high or low frequencies. The estimated error margins calculated for the electrochemical parameters are also presented in this table.

In the case of impedance study, this includes the double-layer capacitance (C_{dl}), adsorption capacity (C_a), and the values of the time constants τ_d and τ_a.

$$C_{dl} = \left(A_d \times R_{ct}^{1-n_d} \right)^{1/n_d} \tag{7}$$

$$C_a = \left(A_a \times R_a^{1-n_a} \right)^{1/n_a} \tag{8}$$

$$\tau_d = R_{ct} \times C_{dl} \tag{9}$$

$$\tau_a = R_a \times C_a \tag{10}$$

The inhibitory efficiency, E%, was calculated from the polarization resistance $\left(R_p = R_{ct} + R_a \right)$ using the following equation (Bentiss *et al.,* 2012):

$$E(\%) = \frac{R_{P(i)} - R_p}{R_{P(i)}} \times 100 \tag{11}$$

where R_p and $R_{p(i)}$ are the polarization resistances of the carbon steel electrode without and with addition of the two compounds, HTMP and DMP, in 1M HCl respectively. The values of

electrochemical parameters and inhibitory efficiency (E%) for different concentrations of HTMP obtained through S.I.E are summarized in **Table 5**.
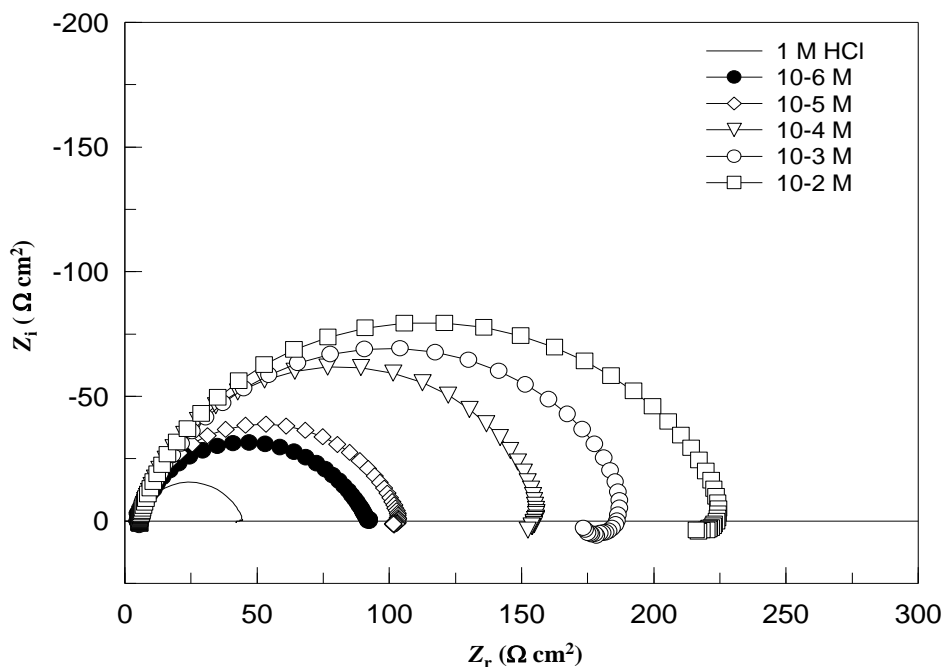

Figure 8. Nyquist diagram of steel in 1M HCl at various concentrations of HTMP at 30°C.
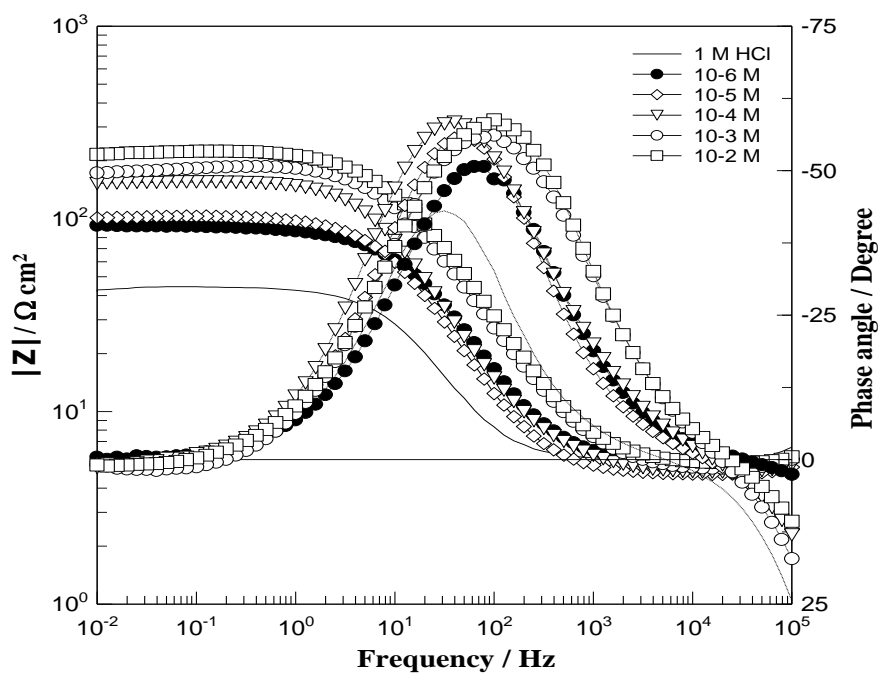

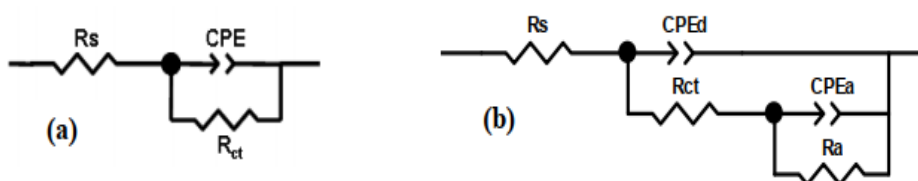**Figure 9.** Bode diagram of steel in 1M HCl at various concentrations of HTMP at 30°C.

Figure 10. Equivalent circuit models for the steel interface in (a) 1M HCl, and (b) HCl + HTMP.
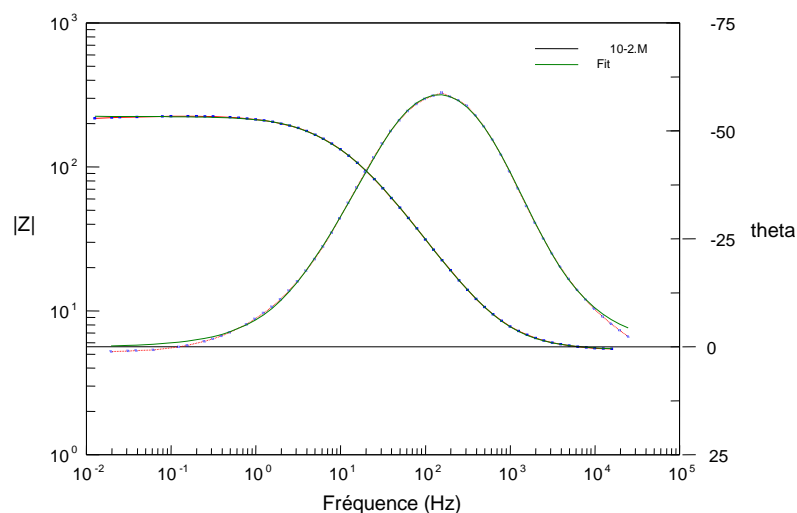
Figure 11. Nyquist representation for the steel interface in a solution of 1M HCl + 1×10^{-2}M HTMP: (---) experimental curve; (---) fitted curve.
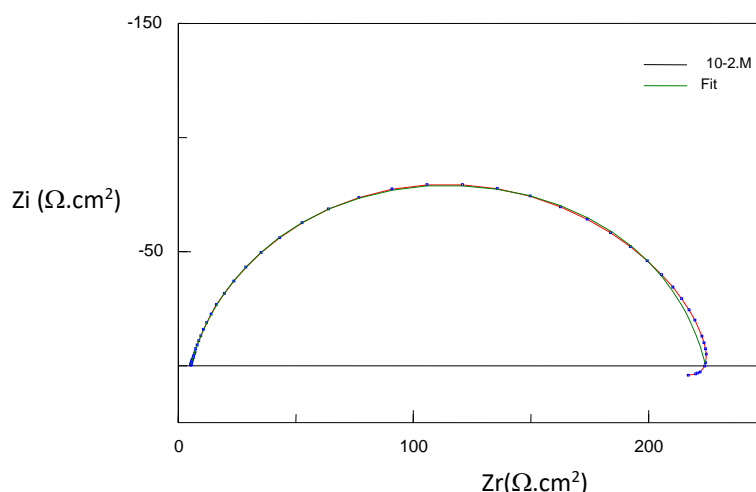

Figure 12. Bode representation for the steel interface in a solution of 1M HCl + 1×10^{-2}M HTMP: (---) experimental curve; (---) fitted curve.

The analysis of these results shows that: **1)** The values of R_{ct} and inhibitory efficiency E (%) increase with the increase in HTMP concentration. **2)** With the addition of HTMP, C_{dl} decreases from 541 µF for the reference to 73.2 µF for HTMP at 10^{-2}M. **3)** The values of Ad are lower than those measured in the absence of HTMP. **4)** The calculated E% values are in agreement with those obtained from gravimetric and polarization measurements. **5)** For the four concentrations studied, HTMP is more effective. This can be attributed to the chemical composition rich in heteroatoms.

It's important to note that the addition of inhibitor in the acidic solution did not affect the values of E_{corr} as well as cathodic Tafel slope, these findings agree the interpretation of Cao, 1996, suggesting that the protection of steel corrosion occurs by the geometric blockage of the metal surface, and thereafter, inhibition efficiency can be estimated using the capacitance:

$$E\%_{Cdl} = \frac{C_{dl}^{blank} - C_{dl}^{inh}}{C_{dl}^{blank}} * 100 \qquad (12)$$

where C_{dl}^{blank} and C_{dl}^{inh} are the capacitance in the absence and presence of inhibitor.

Cao pointed out that, in this case, the inhibition efficiency (η) equals the coverage (θ) of the adsorbed species and can be estimated by polarization resistance (Rp,) measurements. Contrary, if the inhibition is not due to the geometric blocking effect, which can be judged by the noticeable shift of corrosion potential as the inhibitor is added into the solution, then, η cannot be estimated by R_p and does not equal Θ. Instead, transfer resistance (R_t) can always be employed to estimate inhibition efficiency whatever the mode of the inhibition effect. It is argued that theoretically no Tafelian straight lines can be measured in solutions with interface inhibitors unless θ is independent of the electrode potential E or β_a and β_c of the inhibitor changes linearly with E (Cao *et al*., 1996).

Table 5. Electrochemical Parameters and Corrosion Inhibitory Efficiency of Steel in 1M HCl without and with the Addition of Various Concentrations of HTMP at 30°C.

Conc. (M)	R_s (Ω cm²)	R_{ct} (Ω cm²)	$10^4 A_d$ (W⁻¹ sⁿ cm⁻²)	n_d	C_{dl} (μF.cm⁻²)	R_a (Ω cm²)	$10^3 A_a$ (W⁻¹ sⁿ cm⁻²)	n_a	C_a (mF cm⁻²)	R_p (Ω cm²)	E (%)
Blank	5.01 ± 0.02	36.47 ± 0.13	8.70 ± 0.09	0.870 ± 0.001	541.0	—	—	—	—	36.47	—
1×10⁻⁶	4.92 ± 0.01	66.15 ± 0.5	3.45 ± 0.02	0.895 ± 0.001	216.9	-	-	-	—	66.15	44
1×10⁻⁵	4.79 ± 0.03	107.9 ± 0.4	3.17 ± 0.02	0.883 ± 0.005	206.4	-	-	-	—	108	66
1×10⁻⁴	4.97 ± 0.04	153.8 ± 1.8	3.17 ± 0.01	0.849 ± 0.005	182.3	-	-	-	-	154	76
1×10⁻³	5.69 ±0 .012	133.2 ±1.51	1.62 ± 0.01	0.859 ± 0.001	88.9	30.7 ± 1.7	2.57 ± 0.001	0.78 ± 0.02	0.41	164	78
1×10⁻²	5.35 ±0.02	194.6 ± 4.2	1.45 ± 0.02	0.841 ± 0.002	73.2	27;01 ± 1.09	1.45 ± 0.003	0.91 ± 0.07	0.21	221.6	83

3.1.3. Adsorption isotherm

The inhibition of metal corrosion by organic compounds is explained by their adsorption. This process is described by two main types of adsorptions, namely physical adsorption and chemisorption. It depends on the metal's charge, its nature, the chemical structure of the organic product, and the type of electrolyte. The coverage rate (θ) for various inhibitor concentrations in an acidic environment is assessed through electrochemical impedance spectroscopy using the equation:

$$\theta = \frac{R_{ctcor}^{-1} - R_{ctcor(inh)}^{-1}}{R_{ctcor}^{-1}} \tag{13}$$

where R_{ctcor} and $R_{ctcor(inh)}$ represents, respectively, the values of charge transfer resistances of the steel after immersion without and with the addition of the inhibitor.

During this study and in order to find the most significant adsorption isotherm, different types of isotherms were tested, namely Langmuir, Temkin, and Frumkin. These adsorption isotherms have been used for other inhibitors (Bılgıç *et al*., 1999). According to these isotherms, the coverage rate θ is related to the inhibitor concentration C_{inh} by the following equations:

Langmuir adsorption isotherm: $\quad \theta = \dfrac{bC_{inh}}{1+bC_{inh}}$ $\qquad$ (14)

Temkin adsorption isotherm: $\quad \exp(-2a\theta) = KC_{inh}$ $\qquad$ (15)

Frumkin adsorption isotherm: $\left(\dfrac{\theta}{1-\theta}\right)\exp(-2a\theta) = KC_{inh}$ $\qquad$ (16)

where a is a constant representing the interaction between adsorbed particles, b designates the adsorption coefficient, K is the equilibrium constant of the adsorption process, and C_{inh} is the concentration of the inhibitor in the electrolyte. **Table 6** presents the values of θ as a function of the HTMP concentration.

Table 6. Variation of θ with HTMP concentration.

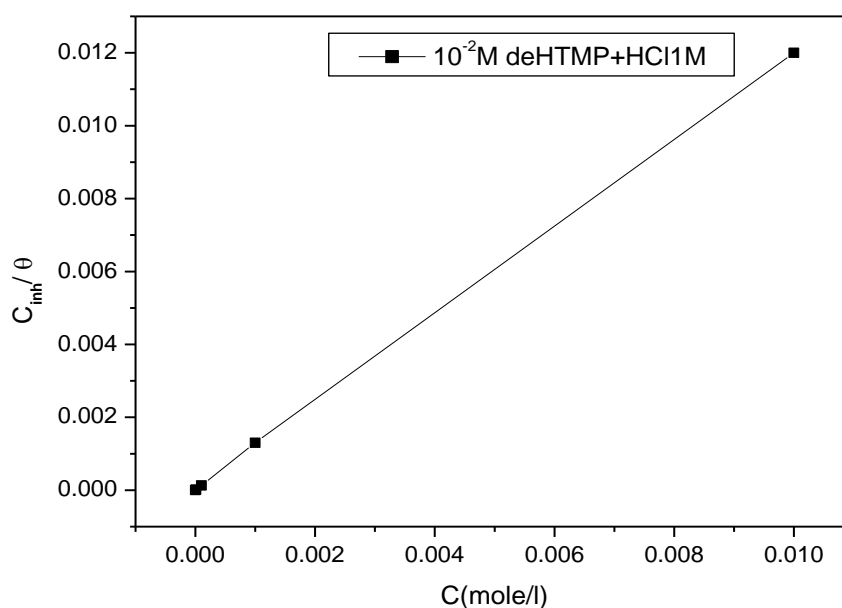| Inhibitor	C(mol /l)	θ
HTMP	10^{-6}	0.44
	10^{-5}	0.66
	10^{-4}	0 .76
	10^{-3}	0.78
	10^{-2}	0.83

Figure 13. Langmuir adsorption isotherm of steel in 1M HCl in the presence of HTMP at 30°C.

In hydrochloric acid medium, the curve of C_{inh}/θ as a function of HTMP concentration is linear (**Figure 13**), indicating that the adsorption of HTMP on the surface of steel in hydrochloric acid follows the Langmuir adsorption isotherm. The calculated standard free energy of adsorption (ΔG_{ads}°) is represented in **Table 7** below.

Table 7. Thermodynamic parameters of HTMP in 1M HCl at 35°C.

Inhibitor	K (M^{-1})	R^2	ΔG$_{ads}$$^{\circ}$ (kJ.mol^{-1})
HTMP	36309,10	0.9999	-36,59

The absolute value of ΔG°_{ads} is greater than 20 kJ/mol (specifically, it is equal to 36.59 kJ/mole for HTMP. This value of ΔG°_{ads} suggests that the adsorption mechanism of HTMP on the surface involves both types of interactions (physisorption and chemisorption), with a predominance of physisorption. Popova *et al.*, 2003 reported that the surface charge of steel at the corrosion potential (E_{corr}) in an HCl medium is positive, initially allowing anions to adsorb. This creates an excess of negative charges on the steel surface, which, in turn, facilitates the physical adsorption of inhibitor cations. Consequently, chlorate and phosphonate ions adsorb on the negatively charged surface (physisorption, $\Delta G^{\circ}_{ads}=-36.59$ kJ/mol). The adsorption of HTMP molecules could occur through the interaction of nitrogen's lone electron pairs and the electrons from the iron atom's d orbital (chemisorption). However, this mode of adsorption makes no substantial contribution. In fact, HTMP molecules in an acidic medium are easily protonated, assuming an ionic form. It is logical to assume that, in this case, the electrostatic adsorption of cations is primarily responsible for the inhibitory properties of HTMP against steel corrosion in HCl medium.

3.2. SEM analysis

SEM observations focused on steel samples after 24 hours of immersion at 30°C in 1M HCl alone then with the addition of concentration 10^{-2}M of HTMP. The examination of the images (SEM) allowed us in particular to highlight the formation of a protective film on the surface of the steel in the presence of HTMP. **Figure 14.a** shows the morphology of the layer formed by the corrosion products after 24 hours of immersion in the 1M HCl solution. We observe black spots on the surface corresponding to corrosion pits, as well as gray and white areas which correspond to oxide films of iron. The **figure 14.b** shows the morphology of the surface of the layer formed after 24 hours of immersion in the 1M HCl solution containing HTMP at concentration (10^{-2}M)
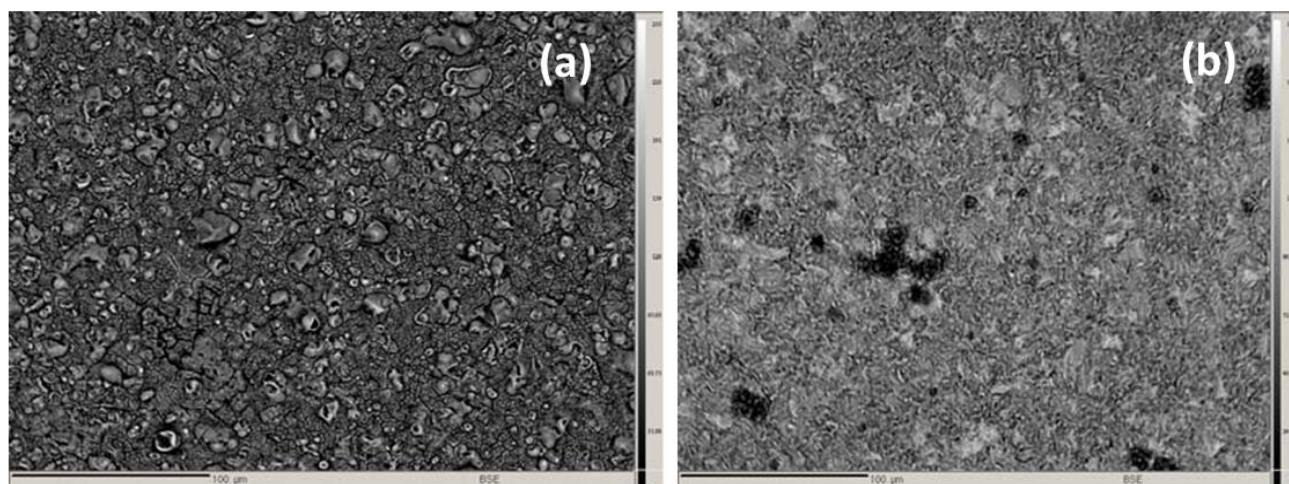

Figure 14. SEM imagines gathered afterward 24 hours of immersion at 30°C in 1M HCl alone (a), and afterward 24 hours of immersion at 30°C in 1M HCl with HTMP(b).

3.3. Theoretical study

3.3.1 DFT tool

The study of the correlation between the inhibitory activity of steel corrosion in 1M HCl and the molecular structure of HTMP is conducted using the Density Functional Theory (DFT) method at the B3LYP level with the 6-31G (d, p) basis set. Quantum chemical indices, namely, the dipole moment

(μ), total energy (TE), Highest Occupied Molecular Orbital (HOMO) and Lowest Unoccupied Molecular Orbital (LUMO) energies, the energy gap (ΔE), and softness (σ), are reported in **Table 8**, and the optimized molecular structure of this compound is illustrated in **Figure 15**. The energy of the Highest Occupied Molecular Orbital (E_{HOMO}) is a quantum chemistry descriptor often associated with a molecule's ability to donate electrons. A molecule with a low energy of the Lowest Unoccupied Molecular Orbital (E_{LUMO}) indicates that its molecular orbitals are vacant. Higher values of E_{HOMO} facilitate the adsorption of the inhibitor onto the metal surface, enhancing inhibitory efficiency by influencing the electron transfer process through the adsorbed layer (Ozcan *et al.,* 2004). The energy of the Lowest Unoccupied Molecular Orbital (E_{LUMO}) of a molecule is associated with its electron-accepting ability: the lower this energy, the greater the likelihood of the molecule accepting electrons. Therefore, a smaller difference in energy (ΔE) between the frontier orbitals of the donor and acceptor leads to higher inhibitory efficiency (as the energy required to remove an electron from the last occupied layer is low).

The results of the obtained quantum parameters indicate that HTMP has a higher HOMO energy value and a low energy gap (ΔE), corresponding to a superior inhibitor. Consequently, this compound possesses a high softness (σ) value and dipole moment, enhancing its inhibitory effectiveness. **Table 8** also illustrates that HTMP has a low total energy, implying that its adsorption occurs easily.
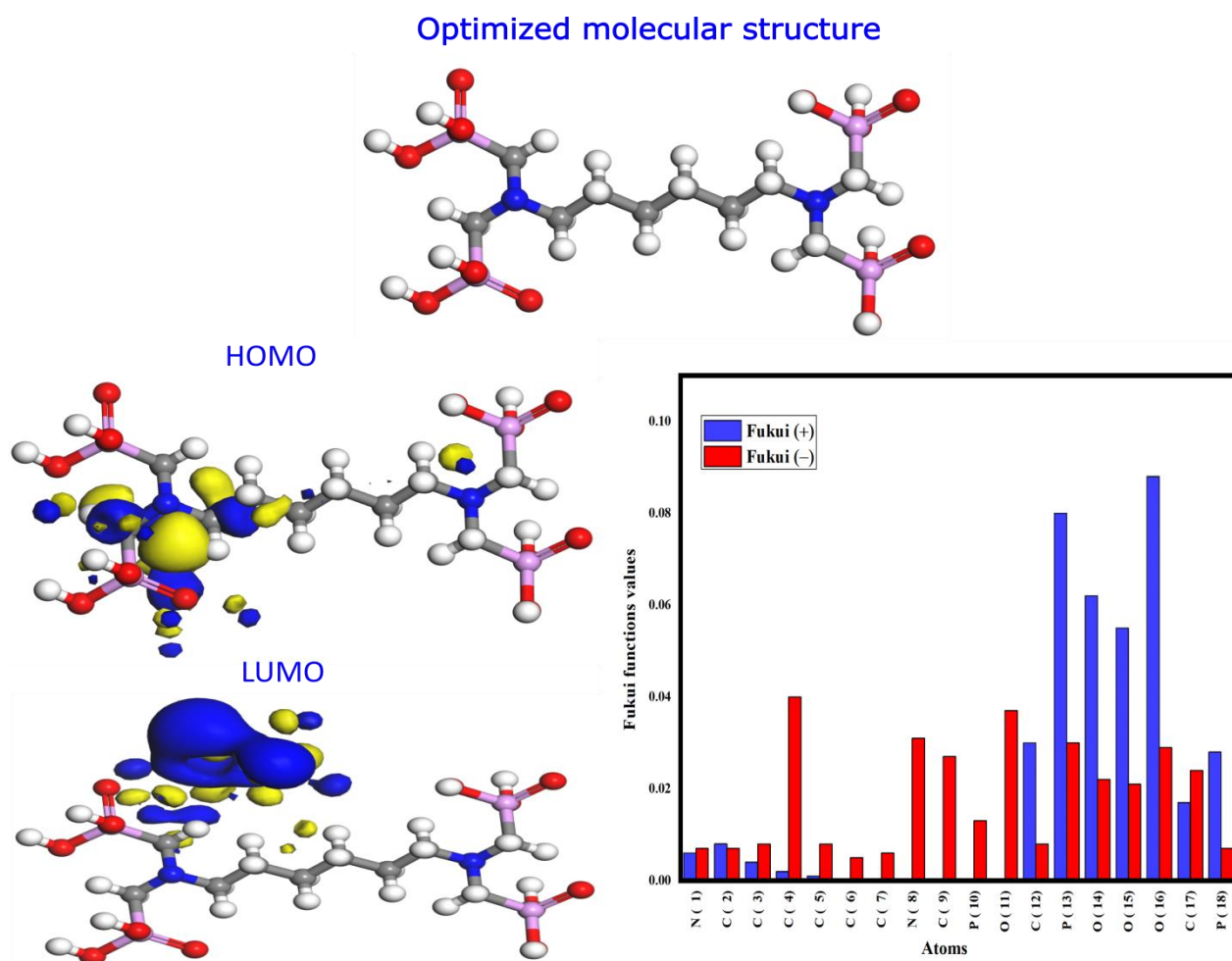

Figure 15. Optimized Molecular Structure, HOMO and LUMO of the HTMP Inhibitor. Fukui indices values for nucleophilic and electrophilic

Table 8. Quantum Parameters of HTMP and their Inhibitory Efficiencies.

Quantum Parameters	HTMP
E_{HOMO} (eV)	-6.231
E_{LUMO} (eV)	-0 .870
$\Delta E(gap)$ (eV)	5.36
μ (Debye)	2.412
E%,W/elec	95 / 81
I (eV)	6.231
A (eV)	0.870
χ (eV)	3.550
η (eV)	2.680
σ (eV)	0.373
ΔN	0.643
TE (eV)	-75505.045

The Fukui index outcomes reveal that HTMP exhibit a substantial number of active centers capable of interacting with the iron surface. This underscores the significance of electron donor and acceptor properties in the corrosive solution, amplifying their corrosion protection capabilities. Ultimately, these results validate the experimental findings, affirming that the molecules provide robust protection against mild steel corrosion under the acidic conditions of 1 M HCl.

3.3.2 First-principles DFT calculations

The theoretical examination of the adsorption of inhibitor molecules onto the iron surface involved first-principles Density Functional Theory (DFT) calculations. Employing spin-polarized DFT calculations, we conducted the analysis using the CASTEP code implemented in Materials Studio. The Self-Consistent Charge (SCC) scheme is implemented to account for polarization effects in the system, enhancing the accuracy of intermolecular interactions within the theoretical framework. To ensure precise and dependable outcomes, the CASTEP module was set to "Fine" quality, and a k-points grid of 8x8x8 was employed for Brillouin zone sampling.

Similar to the molecular dynamics simulations, the iron surface was cleaved into a plane and extended to a (5x5) supercell. Conversely, for the partial density of states analysis, inhibitors were positioned at two distinct locations above the steel surface—near the surface and at a 7Å distance. Electronic structure properties were then calculated to provide insights into the adsorption mechanism and the stability of the inhibitor-steel complex (Messali *et al.,* 2023). Before initiating the first-principles DFT calculations, the inhibitor was placed with a planar geometry above the Fe (1 1 0) surface, while the two lower layers of the supercell were fixed to mimic the bulk steel. The interaction energy of the adsorption system was calculated following the formula provided below (equation 11):

$$E_{inter} = E_{Mol/surf} - (E_{surf} + E_{Mol}) \tag{17}$$

where $E_{Mol/sur}$, $E_{surf,}$ and E_{Mol} indicate the total energy of inhibitor- Fe (110), iron surface, and autonomous molecules, respectively.

Figure 16 illustrates the most stable adsorption structure of HTMP on the Fe surface, determined through geometric optimization employing first-principles DFT simulations. Observations reveal that the HTMP adhere to the iron surface in a flat orientation, underscoring the stability and consistency of their adsorption behavior. The molecule predominantly interacts through its oxygen atoms, establishing robust covalent bonds with the iron surface. Evaluating the strength of inhibitor-iron surface interactions through computed adsorption energies (-1.34 eV), HTMP exhibit negative values, indicating exothermic processes and favorable adsorption on the Fe surface. Furthermore, a projected density of state analysis substantiates the strong adsorption behavior of HTMP on the Fe surface (Fig 16), revealing significant overlap between the inhibitor's molecular orbitals and the Fe d-orbitals. These points to a substantial electronic interaction between the inhibitor molecules and the iron surface, reinforcing their stability and potential effectiveness in inhibiting corrosion. In summary, the outcomes of computational simulations, including analyses of adsorption behavior, bonding distances, adsorption energies, and electronic interactions, collectively indicate that HTMP serve as effective inhibitors for carbon steel in 1M HCl corrosive media.
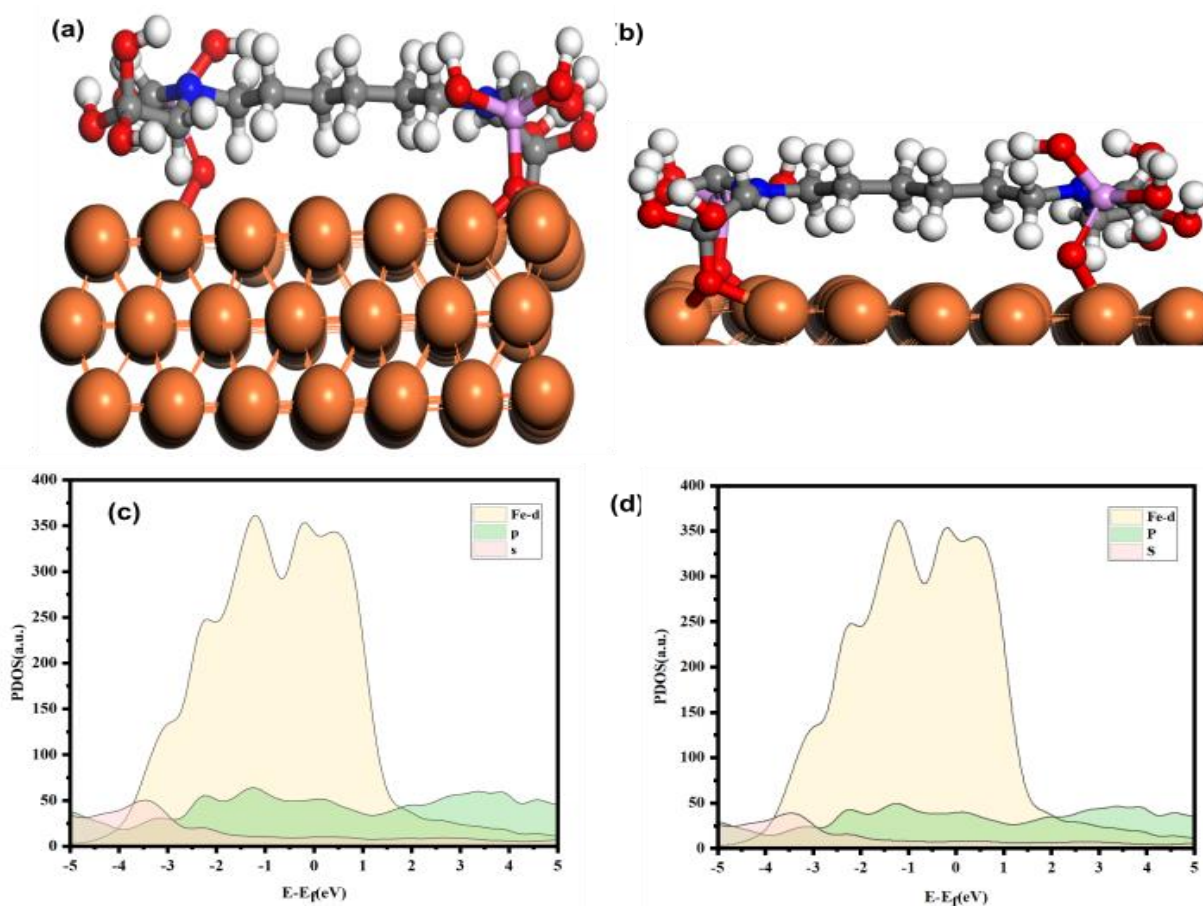

Figure 16: Illustrates the ab inotio DFTB-optimized adsorption structures of HTMP on the Fe(110) surface. Projected Density Of States (PDOS) for HTMP adsorbed on a Fe(110) surface. A Fermi energy point is chosen as a reference for the zero energy state.

3.3.3. Molecular Dynamic (MD) modeling

Molecular Dynamics (MD) simulations offer a robust approach to understanding the interaction forces between organic molecules and metal surfaces in an aqueous environment (Lgaz & al., 2021). In this study, we employed the Forcite computational tool within the Materials Studio software for

conducting molecular dynamics simulations. A pristine iron crystal, oriented along the (110) plane, served as the basis for constructing a 5x5 supercell. The simulation box consisted of three layers of iron atoms and was surrounded by a water box to replicate the HCl solution environment, comprising 500 H_2O molecules, 10 H_3O^+ ions, and 10 Cl^- ions.

The simulations were conducted over a period of 5000 ps, with a time step of 1 fs, utilizing the NVT ensemble in conjunction with the COMPASS force field (Akkermans *& al.,* 2021). Forcite parameters were meticulously adjusted to adhere to "fine" quality specifications.

Figure 17 illustrates the optimized adsorption geometries of the HTMP, which exhibit stability in a parallel arrangement on the Fe (110) surface, as depicted in both top and side views

Upon optimizing the adsorption configuration, molecule of this kind is capable of providing comprehensive surface coverage, influencing the proximity of Fe atoms. Moreover, a deeper understanding of the role of solvent particles enhances our precision in comprehending how these molecules effectively function as corrosion inhibitors. In simpler terms, inhibitor molecules align parallel to the iron surface, facilitating penetration. Consequently, a protective layer forms more uniformly over the metal surface, effectively hindering the ingress of detrimental substances, such as Cl^- ions, and thereby reducing corrosion.
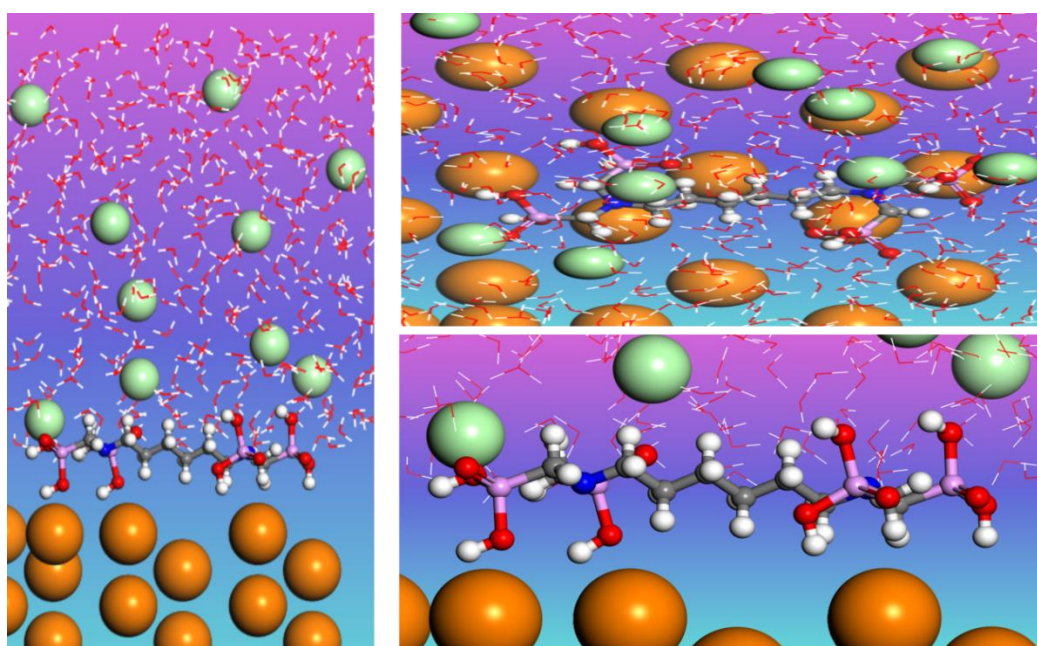

Figure 17: Stable configuration of HTMP in 1M HCl is provided, and molecular dynamics simulations determine these configurations.

Conclusion

The results obtained through the three study methods demonstrate that HTMP is an effective inhibitor, with its inhibition capability increasing with concentration. Other parameters, such as temperature and the immersion time of the steel, may also influence its inhibitory activity. The use of various adsorption isotherms, including Langmuir, Temkin, and Frumkin, revealed that the adsorption of the HTMP inhibitor follows the Langmuir isotherm.

The examination of the images (MEB) allowed us in particular to highlight the formation of a protective film on the surface of the steel in the presence of HTMP.

Analyzing the quantum parameters using the DFT/B3LYP 6-31g(d) method indicates that HTMP has a higher HOMO energy value and a low energy gap (ΔE), making it an excellent inhibitor.

DFTB calculations showed the formation of covalent bonds between inhibitor molecule and iron atoms due to charge transfer, as confirmed by PDOS of adsorbed systems. MD simulations revealed that the HTMP adopted a flat geometry upon adsorption on Fe(11 0) surface, which maximizes the interactions between inhibitors' reactive sites and vacant.

References

Aksüt A.A., Lorenz W.J., Mansfeld F. (1982). The determination of corrosion rates by electro-chemical d.c. and a.c. methods II. Systems with discontinuous steady-state polarization behavior. *Corrosion Science,* 22(7), 611-619. https://doi.org/10.1016/0010-938X(82)90042-7

Amar, H., Benzakour, J., Derja, A., Villemin, D., Moreau, B., & Braisaz, T. (2006). Piperidin-1-yl-phosphonic acid and (4-phosphono-piperazin-1-yl) phosphonic acid: A new class of iron corrosion inhibitors in sodium chloride 3% media. *Applied Surface Science*, 252(18), 6162-6172. https://doi.org/10.1016/j.apsusc.2005.07.073

Amin, M. A., Abd El-Rehim, S. S., El-Sherbini, E. E. F., & Bayoumi, R. S. (2007). The inhibition of low carbon steel corrosion in hydrochloric acid solutions by succinic acid: Part I. Weight loss, polarization, EIS, PZC, EDX and SEM studies. *Electrochimica Acta*, 52(11), 3588-3600. https://doi:10.1016/j.electacta.2006.10.019

Akkermans R.L., Spenley N.A., Robertson S.H. (2021), COMPASS III: Automated fitting workflows and extension to ionic liquids, *Molecular Simulation,* 47, 540– 551.

Ashassi-Sorkhabi, H., Ghalebsaz-Jeddi, N., Hashemzadeh, F., & Jahani, H. (2006). Corrosion inhibition of carbon steel in hydrochloric acid by some polyethylene glycols. *Electrochimica Acta*, 51(18), 3848-3854. https://doi:10.1016/j.electacta.2005.11.002

Askari, F., Ghasemi, E., Ramezanzadeh, B., & Mahdavian, M. (2014). Mechanistic approach for evaluation of the corrosion inhibition of potassium zinc phosphate pigment on the steel surface: Application of surface analysis and electrochemical techniques. *Dyes and Pigments*. https://doi.org/10.1016/j.dyepig.2014.05.024

Azgaou, K., Damej, M., El Hajjaji, S., Sebbar, N. K., Elmselleme, H., El Ibrahimi, B., & Benmessaoud, M. (2022). Synthesis and characterization of N-(2-aminophenyl)-2-(5-methyl-1H-pyrazol-3-yl) acetamide (AMPA) and its use as a corrosion inhibitor for C38 steel in 1 M HCl. Experimental and theoretical study. *Journal of Molecular Structure*, 1266, 133451. https://doi.org/10.1016/j.molstruc.2022.133451

Bammou, L., Chebli, B., Salghi, R., *et al.* (2010). Thermodynamic properties of Thymus satureioides essential oils as corrosion inhibitor of tinplate in 0.5 M HCl: Chemical characterization and electrochemical study. *Green Chemistry Letters and Reviews, 3*(3), 173–178. https://doi.org/10.1080/17518251003660121

Belghiti, M. E., Bouazama, S., Echihi, S., *et al.* (2020). Understanding the adsorption of newly Benzylideneaniline derivatives as a corrosion inhibitor for carbon steel in hydrochloric acid solution: Experimental, DFT and molecular dynamic simulation studies. *Arabian Journal of Chemistry*, 13, 1499–1519. https://doi.org/10.1016/j.arabjc.2017.12.003

Bentiss, F., Outirite, M., Traisnel, M., *et al*. (2012). Improvement of corrosion resistance of carbon steel in hydrochloric acid medium by 3,6-bis(3-pyridyl)pyridazine. *International Journal of Electrochemical Science*, 7, 1699-1723.

Bılgıç, S., & Çalıskan, N. (1999). The effect of N-(1-toluidine) salicylaldimine on the corrosion of austenitic chromium–nickel steel. *Applied Surface Science*, 152(1–2), 107-114. https://doi:10.1016/S0169-4332(99)00308-6

Bouammali H., Jama C., Bekkouch K., *et al.* (2015). Anticorrosion potential of diethylenetriamine-pentakis (methylphosphonic) acid on carbon steel in hydrochloric acid solution. *Journal of Industrial and Engineering Chemistry*, 26, 270–276. doi.org/10.1016/j.jiec.2014.11.039

Bouklah, M., Hammouti, B., Aouniti, A., Benkaddour M., Bouyanzer A. (2006). Synergistic effect of iodide ions on the corrosion inhibition of steel in 0.5 M H_2SO_4 by new chalcone derivatives. *Applied Surface Science,* 252, 6236–6242. doi.org/10.1016/j.apsusc.2005.08.026

Cao C. (1996), On electrochemical techniques for interface inhibitor research, *Corrosion Science,* 38, Issue 12, 2073-2082, ISSN 0010-938X, https://doi.org/10.1016/S0010-938X(96)00034-0

Chkirate, K., Azgaou, K., Elmsellem, H., El Ibrahimi, B., Sebbar, N. K., Anouar, E. H., Benmessaoud, M., El Hajjaji, S., & Essassi, E. M. (2021). Corrosion inhibition potential of 2-[(5-methylpyrazol-3-yl)methyl] benzimidazole against carbon steel corrosion in 1 M HCl solution: Combining experimental and theoretical studies. *Journal of Molecular Liquids*, 321, 114750. https://doi.org/10.1016/j.molliq.2020.114750

Dalmoro, V., Azambuja, D. S., Alemán, C., & Armelin, E. (2019). Hybrid organophosphonic-silane coating for corrosion protection of magnesium alloy AZ91: The influence of acid and alkali pre-treatments. *Surface and Coatings Technology*, 357, 728-739. https://doi.org/10.1016/j.surfcoat.2018.10.013

Dalmoro, V., dos Santos, J. H. Z., Armelin, E., & Alemán, C. (2012). Phosphonic acid/silica-based films: A potential treatment for corrosion protection. *Corrosion Science*, 60, 173-180. https://doi.org/10.1016/j.corsci.2012.03.040

Ech-chihbi, E., Salim, R., Oudda, H., *et al.* (2016). Effect of some imidazopyridine compounds on carbon steel corrosion in hydrochloric acid solution. *Der Pharma Chemica*, 8(13), 214-230.

El Issami S., Bazzi L., Benlhachemi A., Salghi R., Hammouti B., Kertit S. (2007), Triazolic compounds as corrosion inhibitors for copper in hydrochloric acid, *Pigment and Resin Technology,* 36 No 3, 161-168.

Hbika, A., Bouyanzer, A., Jalal, M., *et al*. (2023). The Inhibiting Effect of Aqueous Extracts of Artemisia Absinthium L. (Wormwood) on the Corrosion of Mild Steel in HCl 1 M. *Analytical and Bioanalytical Electrochemistry*, 15(1), 17-35.

Hmamou B. D., Salghi R., Zarrouk A., Zarrok H., Touzani R., Hammouti B., El Assyry A. (2015). Investigation of corrosion inhibition of carbon steel in 0.5 M H_2SO_4 by new bipyrazole derivative using experimental and theoretical approaches. *Journal of Environmental Chemical Engineering*, 3, 2031–2041. https://doi.org/10.1016/j.jece.2015.03.018

Kaur, M., Singh, H., & Prakash, S. (2008). A survey of the literature on the use of high velocity oxy-fuel spray technology for high temperature corrosion and erosion-corrosion resistant coating. Anti-Corrosion Methods and Materials, 55(2), 86-96. https://doi.org/10.1108/00035590810859467

Kedam, M., Mattos, O. R., & Takenouti, H. (1981). Reaction Model for Iron Dissolution Studied by Electrode Impedance: I. Experimental Results and Reaction Model. *Journal of the Electrochemical Society*, 128, 257–266. https://doi:10.1149/1.2127401

Kelly, E. J. (1965). Electrochemical Techniques in Corrosion Science and Engineering, *Journal of The Electrochemical Society*. 112, 125–131. https://doi.org/10.1201/9780203909133

Khamis, E. (1990). The effect of temperature on the acidic dissolution of steel in the presence of inhibitors. *Corrosion*, 46(6), 476–484. https://doi:10.5006/1.3585135

Kinlen, P. J., Ding, Y., & Silverman, D. C. (2002). Corrosion protection of mild steel using sulfonic and phosphonic acid-doped polyanilines. *Corrosion*, 58(6), 490–497. https://doi.org/10.5006/1.3277639

Laamari, R., Benzakour, J., Berrekhis, F., Abouelfida, A., Derja, A., & Villemin, D. (2011). Corrosion inhibition of carbon steel in hydrochloric acid 0.5 M by hexa methylene diamine tetramethyl-phosphonic acid. *Arabian Journal of Chemistry*, 4(3), 271-277. https://doi:10.1016/j.arabjc.2010.06.046

Laamari, R., Benzakour, J., Berrekhis, F., Derja, A., & Villemin, D. (2010). Corrosion inhibition study of iron in sulphuric acid 1M by hexa methylene diamine tetra methyl-phosphonic acid. *Les Technologies de Laboratoire*, 5(20).

Labjar, N., Bentiss, F., Lebrini, M., Jama, C., El Hajjaji, S. (2011). Study of temperature effect on the corrosion inhibition of C38 carbon steel using amino tris(methylenephosphonic) acid in hydrochloric acid solution. *International Journal of Corrosion*. 2011, Article ID 548528, https://doi.org/10.1155/2011/548528

Lazrak, J., Ech-chihbi, E., El Ibrahimi, B., El Hajjaji, F., Rais, Z., Tachihante, M., & Taleb, M. (2022). Detailed DFT/MD simulation, surface analysis and electrochemical computer explorations of aldehyde derivatives for mild steel in 1.0 M HCl. *Colloids and Surfaces A: Physicochemical and Engineering Aspects*, 632, 127822. https://doi.org/10.1016/j.colsurfa.2021.127822

Lebrini, M., Bentiss, F., Chihib, N. E., Jama, C., Hornez, J. P., & Lagrenée, M. (2008). Polyphosphate derivatives of guanidine and urea copolymer: Inhibiting corrosion effect of Armco iron in acid solution and antibacterial activity. *Corrosion Science*, 50(10), 2914-2918. https://doi:10.1016/j.corsci.2008.07.003

Lenderink H. J. W., Linden M.V.D., De Wit, J.H.W. (1993). Corrosion of aluminium in acidic and neutral solutions. *Electrochimica Acta*, 38(14), 1989-1992. https://doi:10.1016/0013-4686(93)80329-X

Liu, F., & Chen, L. (2023). Thiadiazoles as potent inhibitors against corrosion of metals and alloys: Challenges and future prospects. *Journal of Molecular Liquids*, 390(Part A), 122904. https://doi.org/10.1016/j.molliq.2023.122904

Liu, Y., Zhou, X., Lyon, S. B., Emad, R., Hashimoto, T., Gholini, A., Thompson, G. E., Graham, D., & Gibbon, S. R., Francis, D. (2017). An organic coating pigmented with strontium aluminium polyphosphate for corrosion protection of zinc alloy coated steel. *Progress in Organic Coatings*, 102, 29-36. https://doi:10.1016/j.porgcoat.2016.02.020

Lgaz H., Chaouiki A., Lamouri R., Salghi R., Lee H.-S. (2021), Computational Methods of Corrosion Inhibition Assessment, in: Sustainable Corrosion Inhibitors I: Fundamentals, Methodologies, and Industrial Applications, *American Chemical Society*, Chap 6, 87–109. ACS Symposium Series, Vol. 1403 ISBN13: 9780841297906eISBN: 9780841297890 https://doi.org/10.1021/bk-2021-1403.ch006

Mihajlović M. P., Radovanović M. B., Simonović A. T., Tasić Ž. Z., Antonijević M. M. (2019). Evaluation of purine based compounds as the inhibitor of copper corrosion in simulated body fluid. *Results in Physics*, 14, 102357. https://doi.org/10.1016/j.rinp.2019.102357

Morad, M. S. (2000). An electrochemical study on the inhibiting action of some organic phosphonium compounds on the corrosion of mild steel in aerated acid solutions. *Corrosion Science*, 42(8), 1307-1326. https://doi:10.1016/S0010-938X(99)00138-9

Moumeni, O., Chafaa, S., Kerkour, R., Benbouguerra, K., & Chafai, N. (2020). Synthesis, structural and anticorrosion properties of diethyl(phenylamino)methyl)phosphonate derivatives: Experimental and theoretical study. *Journal of Molecular Structure*, 1206, 127693. https://doi.org/10.1016/j.molstruc.2020.127693

Messali, M., Almutairi SM, Ait Mansour A, Salghi R, Lgaz H. (2023) Exploring the mechanisms of eco-friendly pyridinium ionic liquids for corrosion inhibition of carbon steel in saline mediums: Unveiling deeper understanding through experimental and computational approaches. *Journal of Materials Research and Technology,* 27, 8292–8307. doi:10.1016/j.jmrt.2023.11.219

Naderi, R., Mahdavian, M., & Attar, M. M. (2009). Electrochemical behavior of organic and inorganic complexes of Zn(II) as corrosion inhibitors for mild steel: Solution phase study. *Electrochimica Acta*, 54(27), 6892-6895. https://doi.org/10.1016/j.electacta.2009.06.073

Nakayama, N. (2000). Inhibitory effects of nitrilotris(methylenephosphonic acid) on cathodic reactions of steels in saturated Ca(OH)2 solutions. *Corrosion Science*, 42(11), 1897-1920. https://doi.org/10.1016/S0010-938X(00)00034-2

Ozcan, M., Dehri, I., & Erbil, M. (2004). Organic sulphur-containing compounds as corrosion inhibitors for mild steel in acidic media: Correlation between inhibition efficiency and chemical structure. *Applied Surface Science*, 236, 155-164. https://doi:10.1016/j.apsusc.2004.04.017

Popova, A., Sokolova, E., Raicheva, S., & Christov, M. (2003). AC and DC study of the temperature effect on mild steel corrosion in acid media in the presence of benzimidazole derivatives. *Corrosion Science*, 45, 33-58. https://doi:10.1016/S0010-938X(02)00072-0

Prabakaran, M., Vadivu, K., Ramesh, S., & Periasamy, V. (2014). Corrosion protection of mild steel by a new phosphonate inhibitor system in aqueous solution. *Egyptian Journal of Petroleum*, 23(4), 367-377. https://doi.org/10.1016/j.ejpe.2014.09.004

Prabakaran, M., Vadivu, K., Ramesh, S., & Periasamy, V. (2014). Corrosion protection of mild steel by a new phosphonate inhibitor system in aqueous solution. *Egyptian Journal of Petroleum*, 23(4), 367-377. https://doi.org/10.1016/j.ejpe.2014.09.004

Prabakaran, M., Venkatesh, M., Ramesh, S., & Periasamy, V. (2013). Corrosion inhibition behavior of propyl phosphonic acid–Zn2+ system for carbon steel in aqueous solution. *Applied Surface Science*, 276, 592-603. https://doi.org/10.1016/j.apsusc.2013.03.138

Rao, B. V. A., Rao, M. V., Rao, S. S., & Sreedhar, B. (2013). Surface analysis of carbon steel protected from corrosion by a new ternary inhibitor formulation containing phosphonated glycine, Zn2+, and citrate. *Journal of Surface Engineered Materials and Advanced Technology*, 3(1). https://doi:10.4236/jsemat.2013.31005

Raviprabha, K., & Bhat, S. R. (2023). Corrosion inhibition of mild steel in 0.5 M HCl by substituted 1,3,4-oxadiazole. *Egyptian Journal of Petroleum*, 32(2), 1-10. https://doi.org/10.1016/j.ejpe.2023.03.002

Salah, M., Lahcène, L., Omar, A., & Yahia, H. (2017). Study of corrosion inhibition of C38 steel in 1 M HCl solution by polyethyleneiminemethylene phosphonic acid. *International Journal of Industrial Chemistry*, 8, 263–272. https://doi.org/10.1007/s40090-017-0123-2

Salim, R., Nahlé, A., El-Hajjaji, F., Ech-chihbi, E., Benhiba, F., El Kalai, F., Benchat, N., Oudda, H., Guenbour, A., Taleb, M., Warad, I., & Zarrouk, A. (2021). Experimental, Density Functional Theory, and Dynamic Molecular Studies of Imidazopyridine Derivatives as Corrosion Inhibitors for Mild Steel in Hydrochloric Acid. *Surface Engineering and Applied Electrochemistry*, 57, 233–254. https://doi.org/10.3103/S1068375521020083

Sherif, E. M., & Park, S. M. (2006). Effects of 1,4-naphthoquinone on aluminum corrosion in 0.50 M sodium chloride solutions. *Electrochimica Acta*, 51(7), 1313-1321. https://doi:10.1016/j.electacta.2005.06.018

Solmaz, R., Kardaş, G., Çulha, M., Yazıcı, B., & Erbil, M. (2008). Investigation of adsorption and inhibitive effect of 2-mercaptothiazoline on corrosion of mild steel in hydrochloric acid media. *Electrochimica Acta*, 53(20), 5941-5952. https://doi:10.1016/j.electacta.2008.03.055

Souissi, N., & Triki, E. (2008). Modelling of phosphate inhibition of copper corrosion in aqueous chloride and sulphate media. *Corrosion Science*, 50(1), 231-241. https://doi.org/10.1016/j.corsci.2007.06.022

Tabti, L., Khelladi, R. M., Chafai, N., Lecointre, A., Nonat, A. M., Charbonnière, L. J., & Bentouhami, E. (2020). Corrosion protection of mild steel by a new phosphonated pyridines inhibitor system in HCl solution. *Advanced Engineering Forum*, 36, 59-75. https://doi:10.4028/www.scientific.net/AEF.36.59

Timoudan, N., Titi, A., El Faydy, M., Benhiba, F., Touzani, R., Warad, I., Bellaouchou, A., Alsulmi, A., Dikici, B., Bentiss, F., & Zarrouk, A. (2023). Investigation of the mechanisms and adsorption of a new pyrazole derivative against corrosion of carbon steel in hydrochloric acid solution: Experimental methods and theoretical calculations. *Colloids and Surfaces A: Physicochemical and Engineering Aspects*. https://doi.org/10.1016/j.colsurfa.2023.132771

Veloz, M. A., & González, I. (2002). Electrochemical study of carbon steel corrosion in buffered acetic acid solutions with chlorides and H_2S. *Electrochimica Acta*, 48(2), 135-144. https://doi:10.1016/S0013-4686(02)00549-2

Yang, Y. F., Scantlebury, J. D., Koroleva, E., Ogawa, O., & Tanabe, H. (2010). A novel anti-corrosion calcium magnesium polyphosphate pigment and its performance in aqueous solutions on mild steel. *ECS Transactions*, 24. https://doi.org/10.1149/1.3453608

(2024) ; https://revues.imist.ma/index.php/morjchem/index